

ANDRZEJ EJCHART

Instytut Biochemii i Biofizyki PAN
 ul. Pawińskiego 5A, 02-106 Warszawa, Poland
 e-mail: aejchart@ibb.waw.pl

Insight into protein dynamics from nuclear magnetic relaxation studies^{*)}

Summary — In the review (63 references) the nuclear magnetic relaxation which is a unique experimental method giving insight into dynamic processes existing in proteins and covering a broad range of time scales was presented. This method, however, is demanding experimentally and theoretically. Experimental methods limited to ^{15}N nuclei are briefly presented and their limitations discussed. Analysis of experimental relaxation data for proteins can be done in the frame of model-free approach or applying spectral density mapping. Both those approaches are difficult for the physical interpretation of results. Besides motional parameters, some structural parameters influence relaxation rates and have to be estimated or determined. Hopefully, many problems connected with the analysis of relaxation data in proteins can be overcome with relaxation measurements at multiple magnetic fields for different isotopes like ^{15}N , ^{13}C , and ^2H .

Key words: nuclear magnetic relaxation, protein dynamics, ^{15}N relaxation in proteins, model-free approach, spectral density mapping.

WGLĄD W DYNAMIKĘ PROTEIN ZA POMOCĄ MAGNETYCZNEJ RELAKSACJI JĄDROWEJ

Streszczenie — W artykule przeglądowym (63 poz. lit.) przedstawiono wykorzystanie magnetycznej relaksacji jądrowej do badania dynamiki cząsteczkowej w białkach. Ograniczając dyskusję do najczęściej w przypadku białek badanego izotopu ^{15}N , omówiono najważniejsze aspekty doświadczalne pomiarów prędkości relaksacji oraz metody ich interpretacji i powiązania z dynamiką cząsteczkową. W przypadku jąder ^{15}N dominują dwa mechanizmy relaksacji, dipolowy i wywołany przez anizotropię ekranowania. W równaniach opisujących prędkości relaksacji dotyczące tych mechanizmów pojawiają się gęstości spektralne, których postać analityczna zależy od przyjętego modelu ruchu. Ponieważ ruchy wektorów N-H w białkach są złożone, więc do ich opisu stosuje się model ogólny (model-free approach) lub wyznacza się bezpośrednio zależność gęstości spektralnych od częstości. Odrębnym problemem jest wyznaczenie parametrów strukturalnych, takich jak uśredniona wiązanie długość wiązania N-H czy wartości własne tensora ekranowania, które mogą zmieniać się w zależności od reszty aminokwasowej. Pomiar prędkości relaksacji własnej i prędkości interferencji dotyczące szeregu jąder występujących w białkach (^{15}N , ^{13}C , ^2H) w wielu polach magnetycznych pozwalają na otrzymanie szczegółowych informacji o dynamice cząsteczek białek.

Słowa kluczowe: magnetyczna relaksacja jądrowa, dynamika białek, relaksacja ^{15}N w białkach, opis bezmodelowy, próbkowanie gęstości spektralnych.

In complex molecular systems like proteins, their structure, function, and dynamics are tightly interconnected. At present, it is widely accepted that intramolecular motions in proteins are one of the key factors determining their biological activity as interactions with ions, ligands, other proteins, and nucleic acids.

Dynamic processes in proteins cover broad range of frequencies, most often quantitatively described as diffusion constants (D), or their reciprocals, correlation times (τ_c) [1]. Besides the rotational diffusion of a whole molecule ($10^{-9} \text{ s} < \tau_c < 10^{-7} \text{ s}$) a variety of intramolecular mo-

tions can be distinguished. Segmental motions and domain movements ($10^{-9} \text{ s} < \tau_c < 10^3 \text{ s}$) involve changes of large regions of a protein molecule and can be studied using such techniques as equilibration, magnetization transfer, lineshape analysis, and nuclear magnetic relaxation in the rotating and laboratory frame, from the slowest to the fastest process, respectively. Local backbone motions and side chain reorientations ($10^{-12} \text{ s} < \tau_c < 10^{-9} \text{ s}$) are usually studied by means of the relaxation in the laboratory frame. Finally, bond vibrations ($\tau_c < 10^{-12} \text{ s}$) are too fast to be quantitatively studied using NMR techniques, but they influence the values of molecular parameters, e.g., dipolar coupling constants, which play an important role in the nuclear magnetic relaxation.

^{*)} Szkoła Spektroskopii NMR.

First reports on the relaxation measurements in proteins were published nearly two decades ago [2, 3] and within this period a great number of reports and reviews on the subject were published [4–13]. Nuclei of two isotopes with $1/2$ nuclear spins, ^{15}N and ^{13}C , have been most often used to monitor the protein dynamics *via* relaxation studies. This requires to solve three complex tasks. First, owing to relatively low sensitivity of NMR spectroscopy, isotopic labelling becomes necessary. At present, hopefully, many efficient methods of protein isotope labelling are available [14]. Next, experimental techniques allowing performing accurate measurements of relaxation parameters and reliable methods of data reduction have to be used. Finally, on the basis of realis-

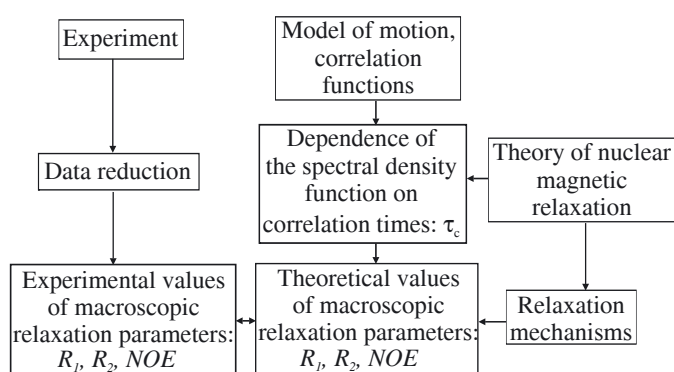


Fig. 1. Scheme of determination of dynamics parameters in molecules from nuclear magnetic relaxation measurements

tic model of motion(s) theoretically reproduced values of experimental relaxation parameters should result in the model parameters characterizing molecular dynamics. Flow chart shown in Fig. 1 presents interrelationships among procedures used for the relaxation measurements and their interpretation in order to elucidate intramolecular dynamics.

In the following text the main attention is focused on the ^{15}N relaxation studies of protein backbone amide nuclei because both, ^{15}N isotopic enrichment and determination of ^{15}N relaxation parameters, are easier and cheaper than for ^{13}C nuclei. On the other hand, ^{13}C relaxation data deliver a unique information of the dynamics of side chains in proteins [7, 15–17]. Relaxation data obtained for quadrupolar ^2H spins in partially deuterated ^{13}C -labeled methyl groups can complement ^{13}C -derived information on the side chain motions [18–21].

EXPERIMENTAL TECHNIQUES AND DATA PROCESSING

Typical ^{15}N relaxation parameters measured in the relaxation studies of proteins are longitudinal ($R_1 = 1/T_1$) and transverse, ($R_2 = 1/T_2$) relaxation rates (inverse of relaxation times) and $^1\text{H}/^{15}\text{N}$ cross-relaxation

rate (σ), the latter being determined *via* nuclear Overhauser effect, $^{15}\text{N}\{^1\text{H}\}$ NOE [10, 11].

$$\text{NOE} = 1 + (\gamma_{\text{H}}/\gamma_{\text{N}})(\sigma/R_1) \quad (1)$$

where: $\gamma_{\text{H}}, \gamma_{\text{N}}$ — appropriate magnetogyric ratios.

It should be pointed out that γ_{N} is negative unlike γ_{H} .

Experimental two-dimensional (2D) techniques of R_1 and R_2 measurements are based on INEPT (Intensive Nuclei Enhanced by Polarization Transfer) from ^1H nuclei to ^{15}N ones and back in order to obtain a maximum possible sensitivity [3]. A typical pulse sequence is composed of the following parts: relaxation delay, refocused INEPT, relaxation period (τ), evolution of ^{15}N chemical shifts (t_1), reverse refocused INEPT, ^1H acquisition (t_2). Set of 2D spectra measured for different relaxation periods τ is used for the determination of appropriate relaxation rates [3].

In the pulse sequence used for R_1 measurements, which is based on the inversion-recovery scheme, relaxation period is sandwiched between two 90° (^{15}N) pulses. Owing to these pulses ^{15}N magnetization is kept along the direction of external magnetic field (z axis) during its evolution. Simultaneous ^1H decoupling is used to suppress the cross-relaxation and interference (cross-correlation) effects [22–24]. The latter arise because ^{15}N nuclei in amides relax due to dipolar (DD) and chemical shift anisotropy (CSA) mechanisms.

R_2 measurements are based on Carr-Purcell-Meiboom-Gill (CPMG) scheme. Relaxation period τ is composed of a train of spin echo sequences, δ — 180 (^{15}N) — δ . In order to minimize the buildup of parasitic antiphase $^1\text{H}_z$ $^{15}\text{N}_x$ coherence owing to scalar coupling between ^1H and ^{15}N nuclei ($^1J_{\text{NH}} \approx 90$ Hz), the condition $2\pi\delta \ll 1$ should be fulfilled [10]. Usually δ is set to *ca.* 600 μs . DD/CSA interference makes an additional relaxation mechanism resulting in biexponential decay of signal intensity *vs.* relaxation period τ . In order to remove the interference effect and retain monoexponential decay 180 (^1H) pulses have to be applied every 5–10 ms.

For NOE determination first INEPT transfer has to be skipped and, therefore, this pulse sequence is *ca.* 10 times less sensitive than the former ones. Magnetization transfer between water protons suppressed by presaturation and amide protons usually causes systematic errors. These errors can be minimized when water presaturation is replaced by flip-back pulses which allow us to keep water magnetization along the external magnetic field [25]. Relaxation delay length in NOE measurements is also of importance [26]. At high magnetic fields DD/CSA interference affects NOE measurements and additional ^1H and ^{15}N pulses are required to suppress this effect [27].

General rules for optimal design and processing of relaxation measurements have been worked out for one-dimensional pulse sequences [28–30] and they remain valid for multidimensional NMR techniques as well. There is, however, a number of factors at all stages of

relaxation data processing of biological molecules which should be especially carefully taken into account due to their strong influence on the accuracy of relaxation parameters [31]. Sufficiently fine spectral digitization, efficient baseline correction, and careful choice of threshold and integration limits during processing of NMR spectra are of special importance. Data reduction leading to the experimental values of relaxation parameters also requires some precaution. Separate R_1 and/or R_2 measurements should be processed together with the use of a multiparameter nonlinear least-squares procedure [32]. Dynamic NOE measurements [33] are preferred over steady-state NOE ones allowing saving total experimental time and improving accuracy. Nevertheless, it has to be stressed that ill-designed and/or ill-performed experiment cannot be saved by applying any sophisticated processing methods. A special care should be taken in the control of temperature. Its stability and consistency in different types of measurements and different spectrometers are crucial for accurate interpretation of experimental data [10, 11].

RELAXATION MECHANISMS AND EQUATIONS DESCRIBING RELAXATION RATES

Two basic relaxation mechanisms taking part in the relaxation of ^{15}N nuclei in protein backbone amide groups are dipolar interaction with amide ^1H spin (DD) and relaxation owing to the ^{15}N chemical shift anisotropy (CSA) [3]. Additionally, the conformational exchange (EX) can contribute to the transverse relaxation rates R_2 [34].

$$R_1 = R_{1,DD} + R_{1,CSA} \quad (2)$$

$$R_2 = R_{2,DD} + R_{2,CSA} + R_{EX} \quad (3)$$

Efficiency of a given relaxation mechanism depends on the amplitude A_n of a n -th interaction and the frequency spectrum of molecular motions expressed in terms of spectral density functions $J(\omega)$:

$$R_{i,n} = A_n^2 \sum_k b_{ik} J(\omega_k) \quad (4)$$

where: subscript i corresponds to the type of relaxation rate, b_{ik} — numerical coefficient.

Basing on the theory of nuclear magnetic relaxation appropriate relaxation rates can be given by the following formulae [35]:

$$R_{1,DD} = \frac{1}{10} D^2 [J(\omega_H - \omega_N) + 3J(\omega_N) + 6J(\omega_H + \omega_N)] \quad (5)$$

$$R_{1,CSA} = \frac{2}{15} C^2 [J(\omega_N)] \quad (6)$$

$$R_{2,DD} = \frac{1}{20} D^2 [4J(0) + J(\omega_H - \omega_N) + 3J(\omega_N) + 6J(\omega_H) + 6J(\omega_H + \omega_N)] \quad (7)$$

$$R_{2,CSA} = \frac{1}{45} C^2 [4J(0) + 3J(\omega_N)] \quad (8)$$

$$R_{EX} = E^2 [J(0)] \quad (9)$$

$$\sigma = \frac{1}{10} D^2 [6J(\omega_H + \omega_N) - J(\omega_H - \omega_N)] \quad (10)$$

It should be reminded that $\gamma_H > 0$ and $\gamma_N < 0$ and, therefore, $\omega_H + \omega_N < \omega_H - \omega_N$. Appropriate amplitudes expressed in [rad/s] are given as:

$$D_{NH} = -\frac{\mu_0}{4\pi} \gamma_H \gamma_N \hbar \left\langle r_{NH}^{-3} \right\rangle \quad (11)$$

$$C_N = \gamma_N B_0 \Delta\sigma \sqrt{1 + \eta^2 / 3} \quad (12)$$

$$E = \gamma_N B_0 \Delta\delta_{AB} \sqrt{p_A p_B} \quad (13)$$

where: $\langle r_{NH}^{-3} \rangle$ is vibrationally averaged N-H distance, $\Delta\sigma = \sigma_{zz} - (\sigma_{xx} + \sigma_{yy})/2$, chemical shift anisotropy and $\eta = 1.5(\sigma_{xx} - \sigma_{yy})/\Delta\sigma$, chemical shift asymmetry, are expressed by the eigenvalues of the shielding tensor σ_{ii} ; $\Delta\delta_{AB}$ — chemical shift difference for the conformational exchange taking place between sites A and B with the rate constant $k_{ex} = k_{A \rightarrow B}/p_B = k_{B \rightarrow A}/p_A$ and p_i are their populations; other symbols have their usual meaning.

It should be pointed out that conformational exchange mechanism is able to influence the transverse relaxation only if $\Delta\delta_{AB} \neq 0$.

Conformational exchange is usually fast in the NMR time scale, i.e., $|\Delta\nu_{AB}| = |10^{-6} \gamma_N B_0 \Delta\delta_{AB}| \ll k_{ex}$, and averaged chemical shifts, $\delta_{av} = p_A \delta_A + p_B \delta_B$ are observed. Therefore, the simultaneous determination of $\Delta\delta_{AB}$, p_A , and $k_{ex} = 1/\tau_{ex}$ becomes unfeasible and only the dependence $R_{EX} \sim B_0^2$ can be utilized. In fact, this dependence justifies the measurements of relaxation rates at multiple magnetic fields. In such a case the R_{EX} term can be presented in more convenient form

$$R_{EX} = \Phi \omega_N^2 \quad (14)$$

where: Φ — frequency independent coefficient [36].

MODELS OF MOTIONS AND SPECTRAL DENSITY FUNCTIONS

Analytical description of spectral density functions appearing in eqs. (5)–(10) is an intricate task because of the complexity of motions in biomolecules. Solely for the isotropic rotational diffusion of a rigid molecule the spectral density function takes a simple form of a single Lorentzian function [35, 37]:

$$J(\omega) = \frac{\tau_R}{1 + \omega^2 \tau_R^2} \quad (15)$$

where: τ_R — rotational correlation time.

The associated diffusion constant is equal $D = 1/6\tau_R$.

Typical dependencies of R_1 , R_2 , and NOE on the τ_R are shown in Fig. 2. Calculations were performed for

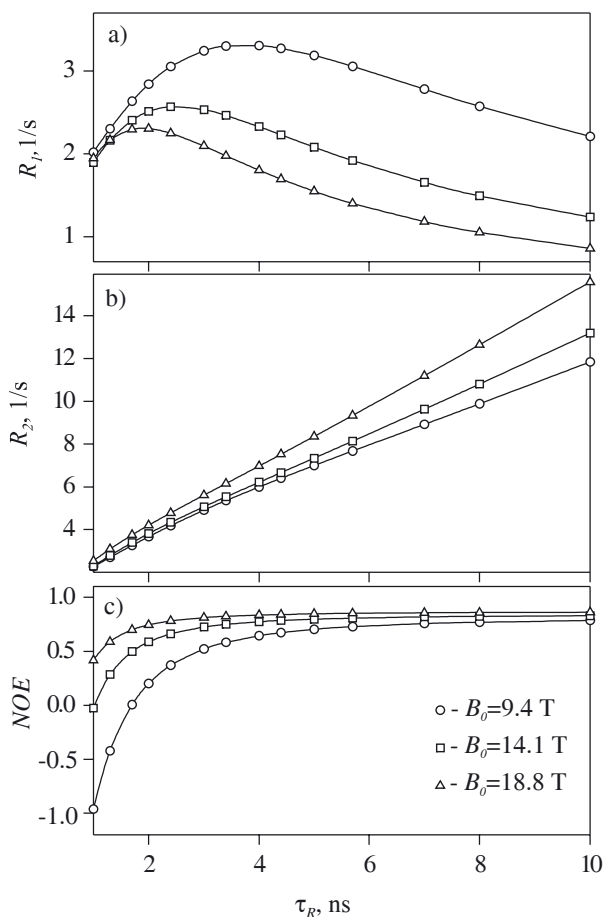


Fig. 2. Longitudinal R_1 (a) and transverse R_2 (b) relaxation rates and nuclear Overhauser effect $^{15}\text{N}\{^1\text{H}\}$ NOE (c) as the functions of rotational correlation time τ_R

three magnetic field strengths (B_0) using Eqs. (1)–(3) and (5)–(10) with spectral density functions given by eq. (15) and it was assumed that $R_{EX} = 0$, $D_{NH} = -6.8 \cdot 10^4$ rad/s, $C_N = -2\pi \cdot 1.6 \cdot 10^{-4} \cdot \gamma_N B_0$ rad/s.

More complex expressions have been derived for the anisotropic rotational diffusion represented by either axially symmetric diffusion tensor or a fully asymmetric one [38]. Then spectral density functions consist of three or five Lorentzian terms, respectively.

Determination of an anisotropic diffusion tensor and its orientation in the molecular frame, which is prone to a number of errors, has been also thoroughly analyzed [39–41].

Since internal motions of backbone amide N-H vectors in proteins are very complex, in the analysis of their relaxation data so-called model-free approach is most often used [42]. It relies on the assumption that rotational diffusion and internal motions are uncorrelated and well separated on the time scale. The rotational diffusion is described by the correlation time τ_R and internal motion(s) by a generalized order parameter (S^2) which is a measure of the degree of spatial restriction of the motion and an effective correlation time (τ_{int}) corresponding to the rate of these motions. For the isotropic

rotational diffusion, model-free approach spectral density function has a form:

$$J(\omega) = \frac{S^2 \tau_R}{1 + \omega^2 \tau_R^2} + \frac{(1 - S^2) \tau}{1 + \omega^2 \tau^2} \quad (16)$$

where: $1/\tau = 1/\tau_R + 1/\tau_{int}$.

Such simple model often fails to represent experimental data accurately, especially NOE values, which tend to exceed the theoretical maximum. In order to overcome this problem an extended model-free approach spectral density function with two internal motions taking place on significantly different time scales has been introduced [43]:

$$J(\omega) = \frac{S^2 \tau_R}{1 + \omega^2 \tau_R^2} + \frac{(1 - S_f^2) \tau_f}{1 + \omega^2 \tau_f^2} + \frac{(S_f^2 - S_s^2) \tau_s}{1 + \omega^2 \tau_s^2} \quad (17)$$

where: S_f , S_s , and τ_f , τ_s — two order parameters and two effective correlation times are associated with fast and slow internal motions, respectively; $S^2 = S_f^2 S_s^2$.

Spectral density functions given by eqs. (16) or (17) can be extended to include anisotropic rotational diffusion [44, 45]. Combination of different types of rotational diffusion with variable number of the model-free parameters results in many descriptions of protein dynamics. Appropriate selection of a model is important for the reliability of the dynamics analysis. Several statistical methods have been proposed for this purpose [46, 47].

SPECTRAL DENSITY MAPPING

The alternative to the model-free approach could be direct determination of the spectral density function dependence on the frequency without using any particular model of motion. Three most often measured relaxation rates given by eqs. (2), (3) and (10) depend on the spectral density functions at five angular frequencies: 0, ω_N , $\omega_H + \omega_N$, ω_H , and $\omega_H - \omega_N$. Therefore, there is not enough experimental data for their determination. Peng and Wagner [48, 49] introduced experimental techniques allowing measurements of longitudinal two-spin order and antiphase transverse coherence relaxation rates which are described by spectral densities at the same frequencies as R_1 , R_2 , and σ . This approach, called spectral density mapping, permits to calculate spectral densities at the five frequencies and has proved to be sensitive to local intramolecular motions [50]. Extension of this method to the measurements at multiple magnetic field strengths results in accurate evaluation of spectral density functions [36].

Despite its virtue the spectral density mapping turned out to be experimentally cumbersome and very prone to experimental error propagation [50]. Observation that the spectral densities vary slowly at high frequencies around ω_H resulted in the modifications of genuine spectral density mapping known as the reduced spectral density mapping. In one approach each of the spectral density values $J(\omega_H + \omega_N)$, $J(\omega_H)$, and $J(\omega_H - \omega_N)$

is replaced with the averaged value $\langle J(\omega_H) \rangle$ [50, 51], whereas in a second one $J(\omega_H + \omega_N)$ is used as a replacement [52, 53]. Another approach [54] bases on the replacement of the linear combinations of spectral densities with a single function according to the following relations:

— in expression defining σ

$$6J(\omega_H + \omega_N) - J(\omega_H - \omega_N) = 5J(0.87\omega_H) \quad (18a)$$

— in expression defining R_1

$$J(\omega_H - \omega_N) + 6J(\omega_H + \omega_N) = 7J(0.921\omega_H) \quad (18b)$$

— in expression defining R_2

$$J(\omega_H - \omega_N) + 6J(\omega_H) + 6J(\omega_H + \omega_N) = 13J(0.955\omega_H) \quad (18c)$$

Assuming that $J(0.87\omega_H) = J(0.921\omega_H) = J(0.955\omega_H)$ two latter values may be replaced by the experimentally derived value of $J(0.87\omega_H)$. Another assumption, $J(\omega) \sim 1/\omega^2$, consistent with a Lorentzian form for the spectral density function leads to the relations:

$$J(0.921\omega_H) = 0.89J(0.87\omega_H) \quad (19a)$$

$$J(0.955\omega_H) = 0.83J(0.87\omega_H) \quad (19b)$$

Despite the fact that the spectral density mapping approach does not require any knowledge concerning the analytical form of spectral density functions, so derived information about protein dynamics shows the same deficiency as model-free approach — it requires the physical interpretation. Moreover, it suffers from the lack of separation of overall and internal motions.

CALCIUM VECTOR PROTEIN — AN EXAMPLE OF RELAXATION DATA ANALYSIS

In calcium vector protein from *Branchiostoma lanceolatum*, CaVP, built up of 161 residues only C-terminal domain (residues 81—161) composed of two EF-hand motifs is functional and binds two Ca^{2+} ions. Structure of this domain in the calcium saturated form (*hollo*) has been determined by means of NMR spectroscopy [55]. Each EF-hand motif is composed of two α -helices sandwiching a calcium binding loop and is rigid in the *hollo* form. Two EF-hand motifs are connected with a flexible linker (residues K116—T123). Secondary structure elements comprise following residues: α -helices, E87—F97, F107—Q115, D124—A134, I144—K152, and a β -strands, V104—D106, V141—D143. Reported ^{15}N relaxation data at four magnetic fields [56] can be used to demonstrate the application of the relaxation measurements for characterizing backbone dynamics with either model-free approach or spectral density mapping.

Model-free approach

If the relaxation data, R_1 , R_2 , and NOE , at a single magnetic field are available, the diffusional correlation time τ_R is usually determined from the R_2/R_1 ratio assuming a simplified form of the spectral density function

given by eq. (15) [3]. Such procedure is valid only if molecular diffusion is isotropic, effective correlation times for internal motions are negligible, there is no conformational exchange, and amplitudes D_{NH} and C_N given by eqs. (11) and (12) are known.

Using the ratios calculated only for the residues located in rigid, secondary structure elements of CaVP one obtains: 1.81 ± 0.09 , 2.46 ± 0.23 , 2.66 ± 0.22 , 3.71 ± 0.30 for B_0 equal 9.4 T, 11.7 T, 14.1 T, and 18.8 T, respectively. Assuming $r_{NH} = 0.102$ nm and $\Delta\sigma = -170$ ppm, these ratios correspond to τ_R values: 4.0 ± 0.3 ns, 4.5 ± 0.4 ns, 4.0 ± 0.3 ns, and 3.9 ± 0.2 ns. Fit of the τ_R to four ratios simultaneously results in $\tau_R = 3.95 \pm 0.05$ ns. Dispersion of τ_R values seems to be acceptable.

Continuing analysis of the data measured at a single magnetic field local parameters, S^2 , τ_{int} , and R_{ex} can be calculated for each residue separately using a formerly obtained τ_R value and substituting spectral density function described by eq. (15) into eqs. (5—10). Results obtained from the data measured at different magnetic fields are not always consistent owing to different τ_R values and variable accuracy of measurements. For instance, S^2 values for the residue 103 are equal to 0.63, 0.80, 0.87, and 0.79 for B_0 equal 9.4 T, 11.7 T, 14.1 T, and 18.8 T, respectively. Therefore, simultaneous fit of one global parameter τ_R and $3N$ local parameters (N —

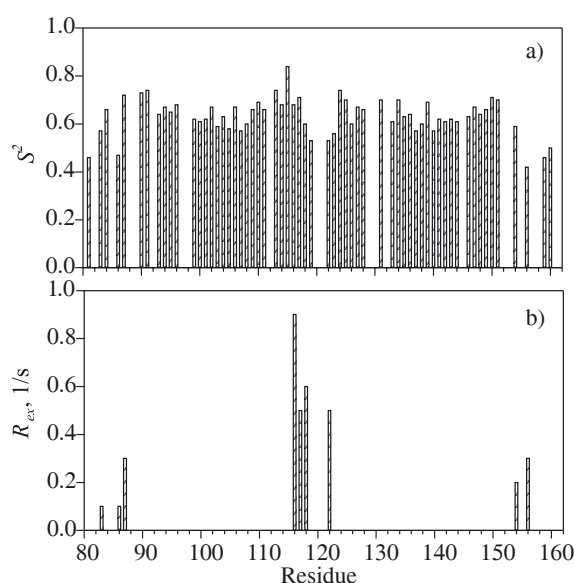


Fig. 3. Model-free parameters for the CaVP obtained from the simultaneous fit to the experimental data reported in Ref. [56] which were measured at B_0 equal 9.4 T, 14.1 T, and 18.8 T: a) order parameters, (S^2), b) exchange terms, (R_{ex}) for $B_0 = 9.4$ T

number of residues) for all available relaxation data is much more reliable. Such calculation performed for the data obtained at four magnetic fields revealed that the measurements at 11.7 T, especially NOEs , were biased due to the systematic error, most probably caused by the temperature shift.

Model-free parameters obtained after rejection of $B_0 = 11.7$ T data are shown in Fig. 3. Order parameters for the residues in the linker and both termini are markedly smaller. Mean values are 0.54, 0.60, and 0.49 for N-terminus, linker, and C-terminus, respectively, as compared with 0.68 for the residues in α -helices. It points out to the increased freedom of fast local motions on the ns—ps timescale. Several residues located in linker and both termini display also relatively slow local motions on the ms— μ s timescale indicated by the R_{ex} term. Diffusional correlation time τ_R obtained in this optimization procedure is equal to 4.8 ns showing that the R_2/R_1 ratio method may significantly underestimate τ_R value.

Spectral density mapping

Spectral density mapping can be performed substituting eqs. (18) and (19) into eqs. (5—10). Values of spectral density function, $J(\omega_N)$ and $J(0.87\omega_H)$, are calculated from the appropriate R_1 and NOE data for each residue at each magnetic field. Determination of $J(0)$ value depends on the number of relaxation data.

If the relaxation data at single magnetic field are only available, $J(0)_{eff}$ can be calculated from the R_2 value and

earlier determined $J(\omega_N)$ and $J(0.87\omega_H)$ according to equation:

$$J(0)_{eff} = J(0) + \lambda R_{ex} \quad (20)$$

where: $\lambda = 45/(9D_{NH}^2 + 4C_N^2)$ [36].

If the data at several magnetic fields are available, $J(0)$ and R_{ex} can be fitted simultaneously using sets of R_2 , $J(\omega_N)$, and $J(0.87\omega_H)$ values.

The latter approach has been applied to analyze relaxation data for CaVP. Similarly like for the model-free analysis it has been found that data obtained for $B_0 = 11.7$ T should be rejected because the reproducibility of R_2 values has been unacceptable. Values of spectral density functions at selected angular frequencies are shown in Fig. 4. $J(0)$ and $J(\omega_N)$ values for both termini and the linker are smaller than the average. On the contrary, $J(0.87\omega_H)$ values for those parts of CaVP are higher than the average. It can be better seen in Fig. 5 displaying

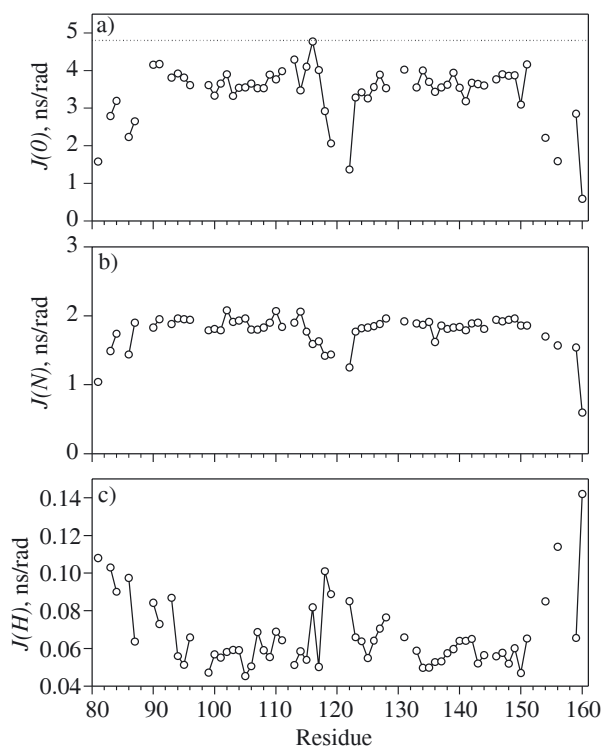


Fig. 4. Results of the spectral density mapping for the CaVP: a) spectral densities at $\omega = 0$. $J(0)$ obtained from the fit of three $J(0)_{eff}$ values calculated from R_2 relaxation rates at B_0 equal 9.4 T, 14.1 T, and 18.8 T according to eq. (20); dotted horizontal line represents a rigid body limit for $J(0)$ — 4.8 ns equal to the diffusional correlation time τ_R [51]; b) spectral densities at $\omega_N = 2\pi \cdot 10^7$ rad/s corresponding to ^{15}N Larmor frequency at $B_0 = 9.4$ T; c) spectral densities at $\omega = 2\pi \cdot 3.5 \cdot 10^8$ rad/s corresponding to 0.87 of ^1H Larmor frequency at $B_0 = 9.4$ T

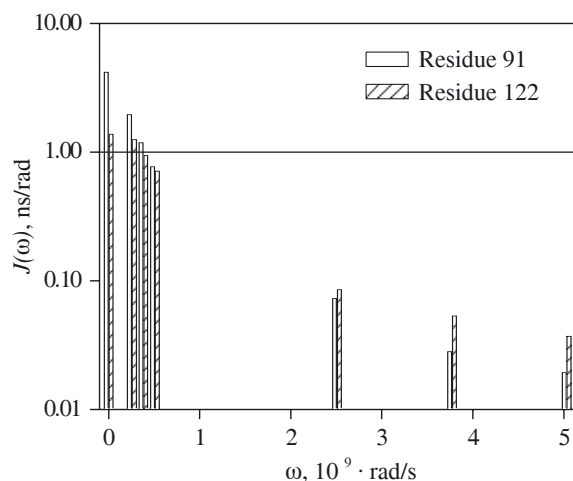


Fig. 5. Spectral density profiles for residue 91 located in a rigid part of CaVP (strongly restricted local motions of N-H vectors) and for residue 122 located in a flexible linker (weakly restricted local motions of N-H vectors)

spectral density profiles for residue 91 located in α -helix and residue 122 from the linker. Parts of the protein that display unrestricted motions are characterized by small values of $J(0)$ and $J(\omega_N)$ and high values of $J(0.87\omega_H)$ [51]. Therefore, results obtained from the spectral density mapping are in agreement with those from the model-free approach. R_{ex} values, although differ from those obtained in the model-free approach, also appear in the flexible parts of molecule.

AMPLITUDES OF RELAXATION MECHANISMS

Efficiency of relaxation mechanism depends on the strength of a spin interaction with surrounding. The dipolar relaxation rates depend on the dipolar constants D_{NH} which in turn depend on the vibrationally averaged N-H distances. Relaxation rates owing to the ^{15}N chemical shift

anisotropy are determined by the eigenvalues of the ^{15}N shielding tensor. It has been usually assumed that these molecular parameters governing relaxation are approximately constant and can be determined with other spectroscopic techniques [3, 57–59]. On the other hand, it has been found that site-specific variations in σ_{ii} [60–62] and r_{NH} [10] values for ^{15}N nuclei can be expected.

Problem with the lack of knowledge of site-specific values of D_{NH} and C_{N} constants in proteins can be overcome with relaxation measurements at multiple magnetic fields. Relaxation data obtained at three or four magnetic fields allow determination of dynamic parameters (correlation times or diffusion constants) and NMR relevant structural parameters (dipolar constants, chemical shift anisotropy) at the same time.

PERSPECTIVES

Nuclear magnetic relaxation measurements of auto and cross-relaxation rates for a variety of nuclei, ^{15}N , ^{13}C , ^2H , at multiple magnetic fields [56, 61, 63] make possible the investigations of conformational dynamics over a wide range of time scales for biomolecules in order to characterize their stability and biological functions.

REFERENCES

- [1] Torchia D. A.: "Protein Dynamics from NMR Relaxation" in "Encyclopedia of NMR" vol.6, (Eds. Grant D. M., Harris R. K.), John Wiley, Chichester 1996, p. 3785. [2] Nir-mala N. R., Wagner G.: *J. Am. Chem. Soc.* 1988, **110**, 7557. [3] Kay L. E., Torchia D. A., Bax A.: *Biochemistry* 1989, **28**, 8972. [4] Wagner G.: *Curr. Opin. Struct. Biol.* 1993, **3**, 748. [5] Palmer A. G.: *Curr. Opin. Struct. Biol.* 1998, **7**, 732. [6] Fischer M. W. F., Majumdar A., Zuiderweg E. R. P.: *Prog. Nucl. Magn. Reson. Spectrosc.* 1998, **33**, 207. [7] Engelke J., Rüterjans H.: "Recent Developments in Studying the Dynamics of Protein Structures from ^{15}N and ^{13}C Relaxation Time Measurements" in "Biological Magnetic Resonance" vol. 17, (Eds. Rama Krishna N., Berliner L. J.), Kluwer/Plenum, New York 1999, p. 357. [8] Ejchart A.: "Relaksacja jądrowa w badaniach dynamiki szkieletów białek" in "Zjawiska relaksacji molekularnej" (Eds. Hawranek J. P., Sobczyk L.), Wyd. Uniwersytetu Wrocławskiego, Wrocław 1999, p. 117. [9] Ishima R., Torchia D. A.: *Nature Struct. Biol.* 2000, **7**, 732. [10] Korzhnev D. M., Billeter M., Arseniev A. S., Orekhov V. Y.: *Prog. Nucl. Magn. Reson. Spectrosc.* 2001, **38**, 197. [11] Fushman D.: "Determination of Protein Dynamics Using ^{15}N Relaxation Measurements" in "BioNMR in Drug Research" (Ed. Zerbe O.), Wiley-VCH, Weinheim 2003, p. 283. [12] Palmer A. G.: *Chem. Rev.* 2004, **104**, 3623. [13] Atkinson R. A., Kieffer B.: *Prog. Nucl. Magn. Reson. Spectrosc.* 2004, **44**, 141. [14] Lian L.-Y., Middleton D. A.: *Prog. Nucl. Magn. Reson. Spectrosc.* 2001, **39**, 171. [15] Nicholson L. K., Kay L. E., Baldissari D. M., Arango J., Young P. E., Bax A., Torchia D. A.: *Biochemistry* 1992, **31**, 5253. [16] Mispelner J., Lefevre C., Adjadj E., Quiniou E., Favaudon V.: *J. Biomol. NMR* 1995, **5**, 233. [17] Liu W., Zheng Y., Cistola D. P., Yang D.: *J. Biomol. NMR* 2003, **27**, 351. [18] Flynn P. F., Bieber Urbauer R. J., Zhang H., Lee A. L., Wand A. J.: *Biochemistry* 2001, **40**, 6559. [19] Walsh S. T., Lee A. L., DeGrado W. F., Wand A. J.: *Biochemistry* 2001, **40**, 9560. [20] Ishima R., Petkova A. P., Louis J. M., Torchia D. A.: *J. Am. Chem. Soc.* 2001, **123**, 6164. [21] Skrynnikov N. R., Millet O., Kay L. E.: *J. Am. Chem. Soc.* 2002, **124**, 6449. [22] Kay L. E., Nicholson L. K., Delaglio F., Bax A., Torchia D. A.: *J. Magn. Reson.* 1992, **97**, 359. [23] Palmer III A. G., Skelton N. J., Chazin W. J., Wright P. E., Rance M.: *Mol. Phys.* 1992, **75**, 699. [24] Skelton N. J., Palmer III A. G., Akke M., Kördel J., Rance M., Chazin W. J.: *J. Magn. Reson. B* 1993, **102**, 253. [25] Grzesiek S., Bax A.: *J. Am. Chem. Soc.* 1993, **115**, 12593. [26] Renner C., Schleicher M., Holak T. A.: *J. Biomol. NMR* 2002, **23**, 23. [27] Gong Q., Ishima R.: *J. Biomol. NMR* 2007, **37**, 147. [28] Weiss G. H., Ferretti, J. A.: *J. Magn. Reson.* 1983, **55**, 397. [29] Weiss G. H., Ferretti J. A., Byrd R. A.: *J. Magn. Reson.* 1987, **71**, 97. [30] Weiss G. H., Ferretti J. A.: *Prog. Nucl. Magn. Reson. Spectrosc.* 1988, **20**, 317. [31] Zhukov I., Ejchart A.: *Acta Biochim. Polon.* 1999, **46**, 665. [32] Gryff-Keller A., Ejchart A., Jackowski K.: *J. Magn. Reson. A* 1994, **111**, 186. [33] Kowalewski J., Ericsson A., Vestin R.: *J. Magn. Reson.* 1978, **31**, 165. [34] Stone M. J., Fairbrother W. J., Palmer III A. G., Reizer J., Saier Jr. M. H., Wright P. E.: *Biochemistry* 1992, **31**, 4394. [35] Abragam A.: "The Principles of Nuclear Magnetism", Oxford University Press, Oxford 1961, Chapter VIII. [36] Peng J. W., Wagner G.: *Biochemistry* 1995, **34**, 16733. [37] Redfield A. G.: *Adv. Magn. Reson.* 1965, **1**, 1. [38] Woessner D. E.: *J. Chem. Phys.* 1962, **37**, 647. [39] Dossset P., Hus J.-C., Marion D.: *J. Biomol. NMR* 2000, **16**, 23. [40] Osborne M. J., Wright P. E.: *J. Biomol. NMR* 2001, **19**, 209. [41] Pawley N. H., Gans J. D., Nicholson L. K.: *J. Biomol. NMR* 2002, **24**, 215. [42] Lipari G., Szabo A.: *J. Am. Chem. Soc.* 1982, **104**, 4536 and 4559. [43] Clore G. M., Szabo A., Bax A., Kay L. E., Driscoll P. C., Gronenborn A. M.: *J. Am. Chem. Soc.* 1990, **112**, 4989. [44] Fan P., Li M. H., Brodsky B., Baum J.: *Biochemistry* 1993, **32**, 13299. [45] Tjandra N., Feller S. E., Pastor R. W., Bax A.: *J. Am. Chem. Soc.* 1995, **117**, 12562. [46] Mandel A. M., Akke M., Palmer A. G.: *J. Mol. Biol.* 1995, **246**, 144. [47] d'Auvergne E. J., Gooley P. R.: *J. Biomol. NMR* 2003, **25**, 25. [48] Peng J. W., Wagner G.: *J. Magn. Reson.* 1992, **98**, 308. [49] Peng J. W., Wagner G.: *Biochemistry* 1992, **31**, 8571. [50] Lefevre J.-F., Dayie K. T., Peng J. W., Wagner G.: *Biochemistry* 1996, **35**, 2674. [51] Wyss D. F., Dayie K. T., Wagner G.: *Protein Sci.* 1997, **6**, 534. [52] Ishima R., Nagayama K.: *J. Magn. Reson. B* 1995, **108**, 73. [53] Ishima R., Nagayama K.: *Biochemistry* 1995, **34**, 3162. [54] Farrow N. A., Zhang O., Szabo A., Torchia D. A., Kay L. E.: *J. Biomol. NMR* 1995, **6**, 153. [55] Thérét I., Baladi S., Cox J. A., Sakamoto H., Craescu C. T.: *Biochemistry* 2000, **39**, 7920. [56] Thérét I., Cox J. A., Mispelner J., Craescu C. T.: *Protein Sci.* 2001, **10**, 1393. [57] Case D. A.: *J. Biomol. NMR* 1999, **15**, 95. [58] Ottinger M., Bax A.: *J. Am. Chem. Soc.* 1998, **120**, 12334. [59] Hiyama Y., Niu C., Silverton J. V., Bavoso A., Torchia D. A.: *J. Am. Chem. Soc.* 1988, **110**, 2378. [60] Fushman D., Tjandra N., Cowburn D.: *J. Am. Chem. Soc.* 1998, **120**, 10947. [61] Fushman D., Tjandra N., Cowburn D.: *J. Am. Chem. Soc.* 1999, **121**, 8577. [62] Fushman D., Cowburn D.: *Methods Enzymol.* 2001, **339**, 109. [63] Canet D., Barthe P., Mutzenhardt P., Roumestand C.: *J. Am. Chem. Soc.* 2001, **123**, 4567.